

## Exotic Behavior of Hydrogen Atoms in Solid H<sub>2</sub> at Temperatures below 1 K

J. Ahokas,<sup>1</sup> J. Järvinen,<sup>1</sup> V. V. Khmelenko,<sup>2</sup> D. M. Lee,<sup>2</sup> and S. Vasiliev<sup>1,\*</sup>

<sup>1</sup>*Wihuri Physical Laboratory, Department of Physics, University of Turku, 20014 Turku, Finland*

<sup>2</sup>*Laboratory of Atomic and Solid State Physics, Cornell University, Ithaca, New York 14853, USA*

(Received 19 April 2006; revised manuscript received 4 July 2006; published 31 August 2006)

We present the first magnetic resonance study of atomic hydrogen embedded in solid H<sub>2</sub> films for temperatures 150–900 mK. We found that at  $T \approx 150$  mK average concentrations of H atoms of order  $10^{18} \text{ cm}^{-3}$  are very stable against recombination during two weeks of observations. The distribution of the population of the two lowest hyperfine states is found to be non-Boltzmann, with a very large occupation of the ground state. We consider the possibility of formation in solid H<sub>2</sub> of regions with high local concentrations of H atoms, where collective quantum phenomena might occur.

DOI: 10.1103/PhysRevLett.97.095301

PACS numbers: 67.65.+z, 67.80.Mg, 76.30.-v

Recent observations of nonclassical rotational inertia in solid helium [1] has sparked interest in other quantum systems where quantum collective phenomena might be seen. Atomic hydrogen embedded in solid crystalline H<sub>2</sub> is a promising candidate for such behavior. Fortunately, previous investigations on the stabilization and recombination of H atoms in solid H<sub>2</sub> have provided an excellent foundation for research in this area. Studies of recombinational heating in solid H<sub>2</sub> containing 0.03% T<sub>2</sub> performed at  $0.16 < T < 0.8$  K showed a large increase in the H atom concentration followed by a spontaneous decay [2,3]. Detailed studies of H atom decay in H<sub>2</sub> solids [4–7] via electron spin resonance (ESR) gave values for the recombination rate constant. Larger concentrations of D atoms were achieved in experiments in D<sub>2</sub> matrices containing T<sub>2</sub> molecules [8,9]. An important transport mechanism of H atoms through solid H<sub>2</sub> is via exchange tunneling reactions, which have been studied extensively in pure hydrogen and H<sub>2</sub>-D<sub>2</sub> mixtures [7,10,11]. In the latter case, very high ( $10^{18} \text{ cm}^{-3}$ ) stable concentrations were obtained [12]. Studies of H atoms in solid H<sub>2</sub> at very low temperatures might reveal anomalous effects associated with magnetic ordering transitions or Bose-Einstein condensation (BEC) of the ensemble of H atoms.

In this work, we present the first ESR studies of H atoms in solid H<sub>2</sub> in the temperature range between 150 and 900 mK. We used a novel method of ultraslow deposition to create a solid H<sub>2</sub> film containing atomic hydrogen on the sample cell walls at a temperature of 350 mK [13]. This method provided a very pure sample of H in H<sub>2</sub>. We found that decreasing the temperature led to a significant decrease in the recombination rate of H atoms. At 150 mK, the lowest temperatures of our study, we did not see any decay of H atoms during two weeks of observation. For the first time, we observed via ESR at 4.6 T a nonthermal (non-Boltzmann) population of the two lowest hyperfine states of H atoms. Saturation experiments, hole burning studies, and electron-nuclear double resonance (ENDOR) measurements were used to characterize the behavior of the embedded H atoms.

Experiments were performed in the sample cell (SC) shown in Fig. 1(a), originally used for the studies of a two-dimensional gas of atomic hydrogen adsorbed on the surface of a superfluid <sup>4</sup>He film [14]. Atomic hydrogen gas is generated by an rf discharge in a cryogenic dissociator, and the high field seeking fraction (H↓) is pulled into the sample cell located in a 4.6 T magnetic field. The total flux of atoms entering the SC is  $\approx 2 \times 10^{13} \text{ s}^{-1}$ . Bulk gas densities up to  $2 \times 10^{15} \text{ cm}^{-3}$  can be accumulated in the SC after several hours of filling at a temperature of  $\approx 350$  mK. H↓ atoms in the lowest two hyperfine states *a* and *b* [Fig. 1(b)] are accumulated in equal amounts under these conditions.

The gas of hydrogen atoms, despite being electron spin-polarized, is not stable and decays via recombination. The molecules resulting from recombination appear in highly excited rotational-vibrational states [15]. They relax down to a ground molecular state, which is ortho-H<sub>2</sub> for the *a* + *b* channel and para-H<sub>2</sub> for *a* + *a*. They cross the superfluid helium film, then stick to the wall of the SC, and finally form a layer of solid H<sub>2</sub>. This layer in the experiments with H↓ helps to reduce the decay rate of the sample due to one-

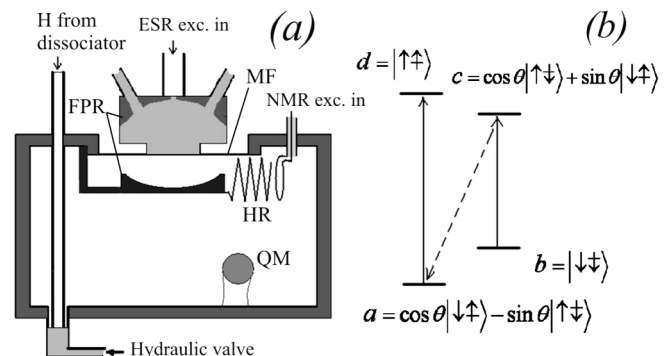


FIG. 1. (a) Schematic drawing of the sample cell. (b) Hyperfine level diagram for a hydrogen atom in a strong magnetic field. FPR = Fabry-Perot ESR resonator, HR = helical NMR resonator, MF = Mylar foil, and QM = quartz microbalance crystal. Arrows denote electron and nuclear spin projections.

body nuclear relaxation. A typical rate for solid H<sub>2</sub> film growth is 0.5–1 molecular layer per hour. We measured the thickness of the solid H<sub>2</sub> film by a quartz microbalance installed inside the SC with a precision better than 1 monolayer. The H<sub>2</sub> film at the end of the coating was found to have a thickness of 150 layers. Surprisingly, we found that a substantial concentration of H atoms was captured inside the solid H<sub>2</sub> film. We believe that atoms were captured after collisions with the excited H<sub>2</sub> molecules in the SC. We verified that the atoms did not diffuse into the sample cell from the dissociator along the solid H<sub>2</sub> film covering the surface of the fill line, since closing the hydraulic valve at the cell bottom stopped the growth of the atomic ESR signal.

The H atoms (contained in the H<sub>2</sub> films) detected by ESR at 128 GHz [16] are situated on the surface of the Mylar foil and on the lower spherical mirror, both located at antinodes of the Fabry-Perot resonator (FPR) operating in the TEM<sub>005</sub> mode. The foil can be actively cooled to a temperature much lower than the rest of the SC. In Fig. 2 (upper left trace), we present the ESR spectra of hydrogen atoms in solid H<sub>2</sub> in the presence of the gas phase. For H atoms in solid H<sub>2</sub>, we observed that the area of the *a-d* line was much larger than that of the *b-c* line (see solid lines on the bottom traces in Fig. 2). A special shim coil is used to minimize the polarizing magnetic field inhomogeneity down to  $\approx 0.2$  G/mm, which defines the width and shape of the lines in Fig. 2. The H  $\downarrow$  in the gas phase can be easily destroyed by lowering the SC temperature down to  $\approx 100$  mK, where the lifetime of the gas sample is several minutes, leaving only H atoms in solid H<sub>2</sub>. The ESR lines of the H in solid H<sub>2</sub> appear to be shifted by  $\approx 0.28$  G towards the center of the spectrum from those of free atoms (see Fig. 2). The magnitude of the shift is the same for both

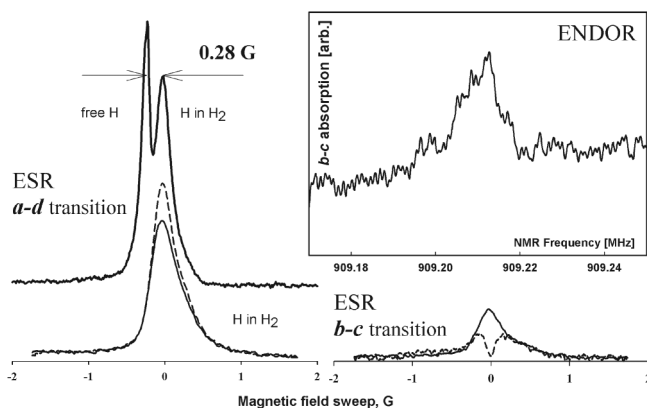


FIG. 2. ESR and ENDOR spectra of H atoms in solid H<sub>2</sub> matrix: Upper left trace shows *a-d* transition of H in solid H<sub>2</sub> (right peak) during sample accumulation at  $T = 350$  mK (left peak is the spectrum of bulk H gas which was introduced into the cell during solid sample formation). Lower traces show the effect of hole burning on the *b-c* ESR line of H atoms in solid H<sub>2</sub> at  $T = 150$  mK: solid lines, before and dashed lines, after hole burning; inset—ENDOR spectrum of H in H<sub>2</sub>.

ESR lines, on the basis of which we conclude that the atoms in the solid have a reduced hyperfine interaction, while the *g* factor is hardly affected.

We also observed the ENDOR spectrum of H atoms as shown in the inset in Fig. 2. For observation of this spectrum, we first saturated the allowed electron *b-c* transition and then swept the frequency (near 909 MHz) of an rf signal applied to the helical NMR resonator (HR) [see Fig. 1(a)] through the position of the nuclear *a-b* transition. Once the nuclear resonance condition is reached, atoms are transferred from the *a* to the *b* state, which leads to an increase of the ESR absorption at the *b-c* transition. From the position of the ENDOR line relative to that of the free atoms, we obtain the value of the hyperfine constant change  $\Delta a/h = -1320(10)$  kHz. The observed reduction of the hyperfine constant with respect to the free atoms implies that the atoms are situated in substitutional sites, where the effects of van der Waals attraction to the neighboring molecules dominate over the Pauli repulsion [17]. The unusually small width of the NMR transition ( $\approx 15$  kHz) may be explained by a motional narrowing effect. The very narrow ENDOR line also provides good evidence that the atoms occupy substitutional sites in our high quality H<sub>2</sub> crystals.

Typically, the H<sub>2</sub> films studied were  $\approx 50$  nm thick and contained  $\approx 50$  ppm of H atoms. We studied the stability of H atoms in solid H<sub>2</sub> at different temperatures. The results of this study are shown in Fig. 3. Only a slow decrease of H atom concentration was observed at 300 and 480 mK. Linearity of the data plots confirms that the decay process is due to the second order recombination of H atoms, with rate constant  $K_r(300 \text{ mK}) = 1.5 \times 10^{-25} \text{ cm}^3/\text{s}$  and  $K_r(480 \text{ mK}) = 3 \times 10^{-25} \text{ cm}^3/\text{s}$ . For these two temperatures, the recombination rate constants  $K_r$  are far smaller

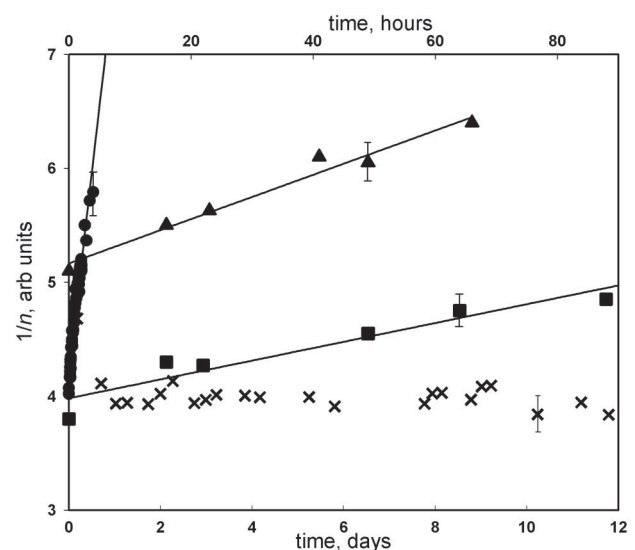


FIG. 3. Decay of H in H<sub>2</sub> sample at different temperatures.  $\times$ ,  $-150$  mK (lower time scale);  $\blacksquare$ ,  $-300$  mK;  $\blacktriangle$ ,  $-480$  mK;  $\bullet$ ,  $-900(50)$  mK (all upper time scale).

than values calculated from the linear dependence of  $K_r$  on  $T$  predicted theoretically [5] and verified in experiments [4] for  $1.35 \leq T \leq 4.2$  K. At 900 mK, the rate constant increased by a factor of  $\approx 20$  compared to  $K_r(480$  mK) and became close to the value obtained by extrapolating results of Ref. [4]. Completely different behavior was observed at 150 mK. At this temperature, the decay of H atoms was imperceptible over a period of at least two weeks. The lack of recombination at the lowest temperatures leads to a vanishingly small heat release, which will make it possible to achieve extremely low temperatures for this metastable system in future experiments. All of the other observations presented in this work were performed at 150 mK, where the concentration of H atoms remained unchanged.

We found that the ESR lines of H in  $H_2$  can be easily saturated by an excitation power of  $\sim 10^{-10}$  W. However, the saturation behavior of the  $a$ - $d$  and  $b$ - $c$  lines is quite different. The  $a$ - $d$  line follows a classical saturation curve as a function of the applied millimeter-wave field  $H_1$  [18] with the maximum at  $H_1 \approx 1.5 \times 10^{-4}$  G. We performed a measurement of this transition relaxation time by recording the recovery of the ESR signal at small power following a saturating pulse at high excitation. We obtained the relaxation time of the  $a$ - $d$  transition  $T_{da} = 3.4(5)$  s. A similar procedure failed to work for the  $b$ - $c$  line. Saturation of this line with high excitation leads to a permanent decrease of the line area. Concomitantly, the area under the  $a$ - $d$  line increased by the same amount as the area under the  $b$ - $c$  line decreased. This effect can be caused by cross relaxation through the forbidden  $c$ - $a$  transition (the Overhauser effect), which was observed previously for H in  $H_2$  at  $T \sim 1.3$  K [19]. By measuring the destruction of the  $b$ - $c$  line at high enough values of the ESR excitation power (so that the destruction rate no longer depends on the ESR

power), we extract the relaxation time of the forbidden  $c$ - $a$  transition  $T_{ca} \leq 5$  s, i.e., about the same as  $T_{da}$ . This is a surprising result, since the expected relaxation rate of the forbidden transition should be a factor of  $\sim \kappa^m$  smaller than that of the allowed transitions, with  $\kappa = 3 \times 10^{-3}$  being the hyperfine mixing parameter and  $m \geq 1.4$  [20].

Using the Overhauser effect, we are able to completely depopulate the  $b$  state and then, by measuring the recovery of the nuclear polarization  $p \equiv (n_a - n_b)/(n_a + n_b)$  to a steady state, we can determine the nuclear relaxation time  $T_{ba}$ . Results of such measurements are shown in Fig. 4. From the exponential fit to the data, we obtain  $T_{ba} = 60$ –80 h. A most intriguing observation in this experiment is that the steady state value of the nuclear polarization  $p(t \rightarrow \infty) = 0.5(1)$  at  $T = 150$  mK is much larger than  $p \approx 0.14$  dictated by the Boltzmann statistics with  $n_a/n_b = \exp(E_{ab}/T)$ , where  $E_{ab} \approx 43$  mK is the energy difference between the  $b$  and  $a$  states. The same value of  $p \sim 0.5$  was also observed immediately following the deposition of the sample, provided that the system was not disturbed by ESR or NMR sweeps at high power.

Applying rf power to the HR, we tried to saturate the  $a$ - $b$  transition to obtain equal populations of the two lowest hyperfine states. This was not expected to be difficult, since we measured precisely the transition frequency from the ENDOR experiment. Furthermore, the relaxation time  $T_{ba}$  is very long ( $\approx 60$ –80 h). In normal NMR studies, one associates a long  $T_1$  with ease of saturation. In our case, we were only able to observe a decrease of the population ratio after intense rf irradiation, which could only attain  $p \approx 0.2$  after  $\sim 500$  s of pumping. Further increase of rf power by more than 10 db did not lead to any further decrease of  $p$  even after several hours of pumping time. In this way, we could obtain the lowest value of  $p$  and then allow it to relax to a steady state (Fig. 4), which turned out to be close to the non-Boltzmann value of  $p \approx 0.5$  corresponding to an  $n_a/n_b$  ratio  $\approx 3$  obtained for the above described relaxation, starting with a high value of  $p$ .

Recovery of the nuclear polarization can be caused by the nuclear spin relaxation and/or by the diffusion of atoms from unperturbed regions. To reveal the role of diffusion, we performed a classical hole burning experiment on the inhomogeneously broadened  $b$ - $c$  line. We used either a small gradient  $\nabla B \approx 1$  G/cm (see bottom traces in Fig. 2) or a much larger gradient  $\nabla B \approx 9$  G/cm. The recovery time of the holes in both cases turned out to be close to the relaxation time of the  $a$ - $b$  transition found from the data in Fig. 4. Therefore, we conclude that nuclear relaxation dominates over diffusion. This gives an upper bound estimate for the spatial diffusion coefficient  $D_{sp} \leq d^2/\tau \approx 10^{-8}$  cm<sup>2</sup>/s, with  $d \approx 0.2$  mm being the spatial size of the hole, and  $\tau \approx 4 \times 10^4$  s the time of observation. The width of the hole  $\Delta B \approx 0.1$  G provides an estimate of the transverse electron relaxation time  $T_{2e} \sim 1/\gamma_e \Delta B \sim 6 \times 10^{-7}$  s. On the other hand, a hole burning experiment applied to the  $a$ - $d$  transition gave a dramatically different

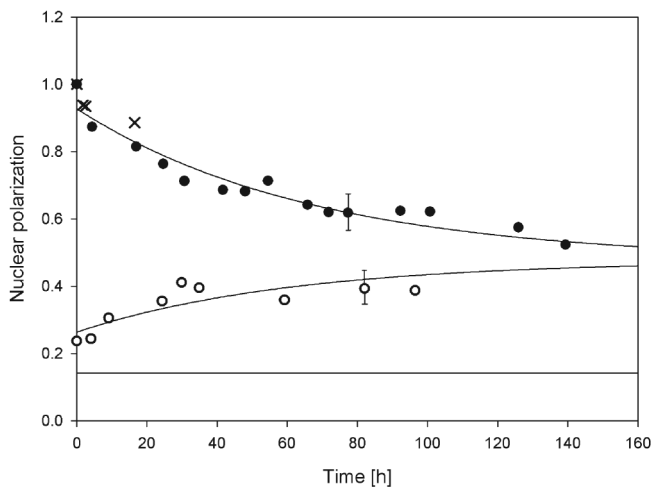


FIG. 4. Evolution of the nuclear polarization  $p = (n_a - n_b)/(n_a + n_b)$  after saturation of the  $b$ - $c$  (●) and  $a$ - $b$  (○) transitions and burning a hole in the  $b$ - $c$  line (×). The horizontal line marks the nuclear polarization corresponding to a thermal (Boltzmann) ratio  $n_a/n_b = \exp(E_{ab}/T)$ , with  $T = 150$  mK.

result. The hole persisted for a very short time, equal to the  $a$ - $d$  relaxation time. ( $\nabla B$  was mainly parallel to the sample surface.)

We suggest possible explanations of the observed phenomena as follows:

(i) *The extremely low recombination rate at 150 mK.*—According to Kumada [21], the motion of H atoms through solid H<sub>2</sub> is dominated by chemical tunneling which involves the reaction  $H + H_2 \rightarrow H_2 + H$ . In order for the atoms to move through the periodic potential of the lattice, the energy levels in successive wells must match each other. As an atom approaches another atom, a mismatch occurs due to a distortion of the crystal [5,11], leading to a disruption in the chemical diffusion.

(ii) *The fast decay of the  $b$  population via the forbidden  $c$ - $a$  transition after saturating the  $b$ - $c$  line.*—Motion of H atoms through the crystal by chemical tunneling reactions may involve intermediate transient states involving a hydrogen atom being loosely bound to a hydrogen molecule for a brief time period. This process may promote  $c$ - $a$  relaxation, allowing pumping of atoms from  $b$  to  $a$  via  $c$ , leading to the buildup of an excess  $a$  population and a depleted  $b$  population, as observed.

(iii) *Anomalous saturation and relaxation behavior of the  $a$ - $b$  transition.*—We suggest that there are two populations of the  $a$  state, one of which saturates easily and the other of which does not saturate. This two population picture is consistent with the exceptionally long lasting large excess population of  $a$  achieved by the pumping action described above. (See Fig. 4.)

(iv) *The large departure from the Boltzmann distribution at  $T = 150$  mK.*—We considered two possibilities to explain this fascinating result. (a) *Magnetic transition via exchange.*—Exchange effects are always a possibility in quantum solids. A magnetic transition could certainly explain a departure from the Boltzmann distribution. We would anticipate that a large frequency shift associated with the growth of an effective internal magnetic field would be seen in the  $a$ - $b$  (NMR) transition. Such a shift was not observed in our experiments. (b) *Statistical correlations associated with BEC.*—This provocative conjecture requires a set of conditions that is difficult to achieve. For a very weakly interacting H gas with a concentration of  $10^{18}$  cm<sup>-3</sup>, corresponding to our average atomic densities, the onset of BEC occurs at about 30 mK. A powerful concentrating mechanism such as the phase separation seen in solid <sup>3</sup>He-<sup>4</sup>He mixtures [22,23] and potentially in ortho-para solid H<sub>2</sub> mixtures [24] is required to reach concentrations of  $\sim 5 \times 10^{20}$  cm<sup>-3</sup>, which corresponds to a BEC onset temperature 0.2 K for an H atom sample with effective mass of  $3.5m_H$ , as calculated from the experimental  $n_a/n_b$  population ratio. Diffusion of the H atoms via exchange can be considered as a motion of “quasivacancies,” leading to a broad energy band and a low effective mass [25]. We might imagine that the H atom rich

phase exists in small bubbles or layers surrounded by the H atom starved phase. Such a model might explain the two populations of state  $a$  inferred from the  $a$ - $b$  relaxation and saturation studies discussed above.

In conclusion, a non-Boltzmann distribution has been observed for the two lowest hyperfine states of H atoms embedded in solid H<sub>2</sub> at temperatures below 1 K perhaps as a result of BEC in regions with high local concentrations of H atoms. High average concentrations of H atoms ( $\sim 10^{18}$  cm<sup>-3</sup>) were stable during two weeks of observation at  $T \sim 150$  mK. Unusual transient magnetic resonance phenomena have been found in this system via saturation studies, hole burning, and ENDOR. Further studies at lower temperatures are needed to help characterize this fascinating system.

This work was supported by the Academy of Finland Grant No. 206109, the Wihuri Foundation, NSF Grant No. DMR 0504683, and NASA Grant No. NAG 3-2871. We also thank K.-A. Suominen, E. Mueller, N. W. Ashcroft, and N. Prokof'ev for extremely useful conversations.

---

\*Electronic address: servas@utu.fi

- [1] E. Kim and M. H. W. Chan, *Science* **305**, 1941 (2004).
- [2] R. W. H. Webeler, *J. Chem. Phys.* **64**, 2253 (1976).
- [3] G. Rosen, *J. Chem. Phys.* **65**, 1735 (1976).
- [4] A. V. Ivliev *et al.*, *JETP Lett.* **36**, 472 (1982).
- [5] Y. Kagan and A. J. Leggett, *Quantum Tunnelling in Condensed Media* (North-Holland, Amsterdam, 1992).
- [6] T. Miyazaki *et al.*, *J. Phys. Chem.* **88**, 4959 (1984).
- [7] T. Miyazaki, *Atom Tunnelling Phenomena in Physics, Chemistry and Biology* (Springer, Berlin, 2004).
- [8] M. Sharno and R. Pound, *Phys. Rev.* **132**, 1003 (1963).
- [9] G. Collins *et al.*, *Phys. Rev. B* **45**, 549 (1992).
- [10] E. B. Gordon *et al.*, *JETP Lett.* **37**, 282 (1983).
- [11] A. V. Ivliev *et al.*, *JETP Lett.* **38**, 379 (1983).
- [12] S. I. Kiselev *et al.*, *Phys. Rev. Lett.* **89**, 175301 (2002).
- [13] S. Vasilyev *et al.*, *Proceedings of the 24th International Conference on Low Temperature Physics* (to be published).
- [14] J. Järvinen *et al.*, *Phys. Rev. A* **72**, 052713 (2005).
- [15] Y. M. Xiao *et al.*, *Phys. Rev. B* **48**, 15744 (1993).
- [16] S. Vasilyev *et al.*, *Rev. Sci. Instrum.* **75**, 94 (2004).
- [17] S. N. Foner *et al.*, *J. Chem. Phys.* **32**, 963 (1960).
- [18] C. P. Poole, *Electron Spin Resonance. A Comprehensive Treatise on Experimental Techniques* (Wiley Interscience, New York, 1967).
- [19] A. Y. Katunin *et al.*, *Phys. Lett.* **87A**, 483 (1982).
- [20] N. V. Prokof'ev and G. V. Shlyapnikov, *Sov. Phys. JETP* **66**, 1204 (1987).
- [21] T. Kumada, *Phys. Rev. B* **68**, 052301 (2003).
- [22] D. O. Edwards *et al.*, *Phys. Rev. Lett.* **9**, 195 (1962).
- [23] V. Maidaev *et al.*, *J. Low Temp. Phys.* **126**, 133 (2002).
- [24] H. Meyer, *Can. J. Phys.* **65**, 1453 (1987); H. Meyer, *Low Temp. Phys.* **24**, 381 (1998).
- [25] D. I. Pushkarov, *Central Eur. J. Phys.* **2**, 420 (2004).